

EoS of finite density QCD with Wilson fermions by Multi-Parameter Reweighting and Taylor expansion

Keitaro Nagata and Atsushi Nakamura

*Research Institute for Information Science and Education, Hiroshima University,
Higashi-Hiroshima 739-8527 Japan*

E-mail: kngt@hiroshima-u.ac.jp, nakamura@riise.hiroshima-u.ac.jp

ABSTRACT: The equation of state (EoS), quark number density and susceptibility at nonzero quark chemical potential μ are studied in lattice QCD simulations with a clover-improved Wilson fermion of 2-flavors and RG-improved gauge action. To access nonzero μ , we employ two methods : a multi-parameter reweighting (MPR) in μ and β and Taylor expansion in μ/T . The use of a reduction formula for the Wilson fermion determinant enables to study the reweighting factor in MPR explicitly and higher-order coefficients in Taylor expansion free from errors of noise method, although calculations are limited to small lattice size. As a consequence, we can study the reliability of the thermodynamical quantities through the consistency of the two methods, each of which has different origin of the application limit.

The thermodynamical quantities are obtained from simulations on a $8^3 \times 4$ lattice with an intermediate quark mass ($m_{PS}/m_V = 0.8$). The MPR and Taylor expansion are consistent for the EoS and number density up to $\mu/T \sim 0.8$ and for the number susceptibility up to $\mu/T \sim 0.6$. This implies within a given statistics that the overlap problem for the MPR and truncation error for the Taylor expansion method are negligible in these regions.

In order to make MPR methods work, the fluctuation of the reweighting factor should be small. We derive the equation of the reweighting line where the fluctuation is small, and show that the equation of the reweighting line is consistent with the fluctuation minimum condition.

KEYWORDS: Lattice QCD, finite density, EoS

Contents

1	Introduction	1
2	Framework	3
2.1	Action and thermodynamical quantities	3
2.2	Multi-parameter reweighting	4
2.3	Overlap problem and reweighting line	5
2.4	Reduction formula for the Wilson fermion determinant	6
2.5	Taylor expansion of EoS	7
3	Result	8
3.1	Simulation setup	8
3.2	Fluctuation of the quark determinant	9
3.3	Fluctuation of the reweighting factor and Reweighting line	11
3.4	Consistency of MPR and Taylor expansion for EoS	12
3.5	Consistency with imaginary chemical potential approach	15
3.6	Finite size effects	15
4	Summary	17

1 Introduction

Thermodynamical properties of strongly interacting matter have been of prime interest in hadron physics. Such an understanding is inevitable to complete the understanding of states of matter such as normal nuclear matter, quark-gluon plasma and dense matters, which are related to the study of evolution of universe, heavy ion collisions, and dense matter inside compact stars.

Lattice QCD is a powerful method to study the non-perturbative nature of QCD. However, the introduction of quark chemical potential μ causes the sign problem for lattice QCD simulations, and standard Monte Carlo(MC) techniques are not applicable for $\mu \neq 0$ [1]. Several methods have been developed to deal with nonzero- μ systems in lattice QCD simulations [1–3].

A reweighting is a general technique for MC simulations to reduce numerical costs [4]. Let us consider a space spanned by parameters of a system. An idea of the reweighting is to perform importance sampling at a point on the parameter space (simulation point), and to calculate observables for other points (target point) by using the samples obtained at the simulation point. The reweighting provides a reweighting factor to compensate the difference of weights between the two points. This method was applied for chemical potential in the Glasgow method [5, 6]. Later Fodor and Katz proposed a method to improve the reweighting method by adopting multiple parameters as shifted

parameters [7], which is referred to as the multi-parameter reweighting (MPR) method. The location of the critical end point and the equation of state was investigated, by using the MPR method with staggered fermions with four-flavor [7] and 2+1 flavor [8–10]. See also Ref. [11].

Although MPR provides a way to investigate QCD at $\mu \neq 0$ by circumventing the breakdown of MC methods, it may encounter problems caused by the fluctuation of the reweighting factor. The fluctuation of the phase of the reweighting factor causes the sign oscillation appearing at the step of the ensemble average of observables. Large phase-fluctuation makes MPR unreliable [12]. On the other hand, large fluctuation of the absolute value causes the decrease of the number of effective samples, which implies less overlap between important configurations at the simulation point and those at the target point.

Another approach to study QCD at $\mu \neq 0$ is to make use of the Taylor expansion at $\mu = 0$, which has been studied in e.g. Refs. [13–17]. The use of the Taylor expansion methods needs a careful investigation on the truncation error of the Taylor series, especially for near and below the pseudo critical temperature T_{pc} .

The two approaches suffer from different systematic errors: the overlap and sign problems for MPR, and the truncation errors for the Taylor expansion. Therefore, it is valuable to study their consistency, which provides a complementary way to confirm the reliability of calculations.

In the present work, we calculate thermodynamical quantities by using MPR and Taylor expansion with a careful attention on their consistency. Although the consistency is empirically known, it is important to show the consistency explicitly in a way free from statistical errors such as noise or truncation errors of Taylor expansion.

We also investigate the validity of MPR. The validity of the MPR method were investigated in detail in Refs. [12, 18] by using staggered fermions. The fermion determinant controls the phase fluctuation of the reweighting factor. Hence, the numerical difficulty of MPR is caused in part by the fluctuation of the fermion determinant. In addition, reweighting lines depend on the parameters of the actions. Hence, it is important to investigate MPR by different fermion actions.

For the purpose, we evaluate the fermion determinant exactly with the use of a reduction formula for Wilson fermions [19–21]. As we will see later, the formula makes it feasible to evaluate the determinant without any approximation. In addition, the formula describes the quark determinant as an analytic function of μ . This feature enables to evaluate the determinant for an arbitrary value of μ , and makes it easy to evaluate higher-order Taylor coefficients. However, note that the determinant evaluation needs large numerical cost even though the reduction formula is used, which imposes the limitation on the applicable lattice size.

This paper is organized as follows. We explain the framework in the next section. The MPR method is introduced in 2.2, the overlap problem and the reweighting line to suppress the overlap problem is discussed in 2.3. The reduction formula is presented in 2.4. Numerical results are shown in section 3. Simulation setup is given in 3.1. Properties of the fermion determinant and reweighting factor is investigated in 3.2 and 3.3. Then, the consistency of MPR and Taylor expansion for EoS et. al. is discussed in 3.4. We also make a comparison with imaginary chemical potential approach in 3.5. Finite size effect on MPR is mentioned in 3.6. The final section is devoted to a summary.

2 Framework

2.1 Action and thermodynamical quantities

The grand partition function of N_f -flavor QCD at a temperature T and quark chemical potential μ is given by

$$Z_{GC}(\mu, T) = \int \mathcal{D}U [\det \Delta(\mu)]^{N_f} e^{-\beta S_G}. \quad (2.1)$$

Here S_G is the RG-improved gauge action divided by β . N_f is the number of the flavors, where we consider $N_f = 2$ in simulations. This definition of S_G is convenient in the MPR method. We employ the clover-improved Wilson fermion

$$\begin{aligned} \Delta(\mu) = & \delta_{x,x'} - \kappa \sum_{i=1}^3 \left[(1 - \gamma_i) U_i(x) \delta_{x',x+\hat{i}} + (1 + \gamma_i) U_i^\dagger(x') \delta_{x',x-\hat{i}} \right] \\ & - \kappa \left[e^{+\mu a} (1 - \gamma_4) U_4(x) \delta_{x',x+\hat{4}} + e^{-\mu a} (1 + \gamma_4) U_4^\dagger(x') \delta_{x',x-\hat{4}} \right] \\ & - \kappa C_{SW} \delta_{x,x'} \sum_{\mu \leq \nu} \sigma_{\mu\nu} F_{\mu\nu}, \end{aligned} \quad (2.2)$$

where κ and C_{SW} are the hopping parameter and clover coefficient. In a homogeneous system, the EoS at T and μ is defined by $p = (T/V_s) \ln Z_{GC}$, which is

$$\frac{p(\mu, T)}{T^4} = \left(\frac{N_t}{N_s} \right)^3 \ln Z_{GC}(\mu, T) \quad (2.3)$$

in the lattice with spatial extent $N_s (= N_x = N_y = N_z)$ and temporal extent N_t . On this lattice $T = (aN_t)^{-1}$ and $V_s = (aN_s)^3$ with a lattice spacing a . In simulations, we consider the deviation of the pressure from $\mu = 0$

$$\frac{\delta p(\mu, T)}{T^4} = \frac{p(\mu, T)}{T^4} - \frac{p(0, T)}{T^4}. \quad (2.4a)$$

The quark number density and quark number susceptibility are given by

$$\begin{aligned} \frac{n}{T^3} &= \frac{\partial}{\partial(\mu/T)} \frac{\delta p}{T^4} \\ &= \left(\frac{N_t}{N_s} \right)^3 \left\langle \frac{(T\partial/\partial\mu)[\det \Delta(\mu)]^{N_f}}{[\det \Delta(\mu)]^{N_f}} \right\rangle, \end{aligned} \quad (2.4b)$$

$$\begin{aligned} \frac{\chi}{T^2} &= \frac{\partial^2}{\partial(\mu/T)^2} \frac{\delta p}{T^4} \\ &= \left(\frac{N_t}{N_s} \right)^3 \left[\left\langle \frac{(T\partial/\partial\mu)^2 [\det \Delta(\mu)]^{N_f}}{[\det \Delta(\mu)]^{N_f}} \right\rangle - \left\langle \frac{(T\partial/\partial\mu) [\det \Delta(\mu)]^{N_f}}{[\det \Delta(\mu)]^{N_f}} \right\rangle^2 \right]. \end{aligned} \quad (2.4c)$$

2.2 Multi-parameter reweighting

To calculate Eqs. (2.4) for $\mu \neq 0$, we employ the MPR method regarding μ and β [7, 18].

The Boltzmann weight

$$w(\mu, \beta) = [\det \Delta(\mu)]^{N_f} e^{-\beta S_G}, \quad (2.5)$$

provides a probability in importance sampling. However, it is unfeasible to update gauge configurations with $w(\mu, \beta)$ for $\mu \neq 0$, because it is in general complex. A basic idea of MPR is to decompose $w(\mu, \beta)$ into two parts as

$$w(\mu, \beta) = R(\mu, \beta)_{(0, \beta_0)} w(0, \beta_0), \quad (2.6)$$

and to perform importance sampling at $(0, \beta_0)$ with $w(0, \beta_0)$ as the probability. The remaining factor $R(\mu, \beta)_{(0, \beta_0)} \equiv w(\mu, \beta)/w(0, \beta_0)$ is instead taken into account at the step of the calculation of observables. R is often called the reweighting factor and reads

$$R(\mu, \beta)_{(0, \beta_0)} = \left(\frac{\det \Delta(\mu)}{\det \Delta(0)} \right)^{N_f} e^{-(\beta - \beta_0) S_G}. \quad (2.7)$$

Note that $R(\mu, \beta)_{(0, \beta_0)}$ is given in terms of configurations obtained at $(0, \beta_0)$. The grand-partition function is rewritten as

$$\begin{aligned} Z_{GC}(\mu, T) &= \int \mathcal{D}U \left(\frac{\det \Delta(\mu)}{\det \Delta(0)} \right)^{N_f} e^{-(\beta - \beta_0) S_G} [\det \Delta(0)]^{N_f} e^{-\beta_0 S_G}, \\ &= \int \mathcal{D}U R(\mu, \beta)_{(0, \beta_0)} w(0, \beta_0). \end{aligned} \quad (2.8)$$

The expectation value of an observable O is given by

$$\begin{aligned} \langle O \rangle &= \frac{\int \mathcal{D}U O R(\mu, \beta)_{(0, \beta_0)} w(0, \beta_0)}{\int \mathcal{D}U R(\mu, \beta)_{(0, \beta_0)} w(0, \beta_0)} \\ &= \frac{\langle O R(\mu, \beta)_{(0, \beta_0)} \rangle_0}{\langle R(\mu, \beta)_{(0, \beta_0)} \rangle_0}. \end{aligned} \quad (2.9)$$

Here $\langle \cdot \rangle_0$ denotes an average taken over an ensemble generated with the importance sampling with the weight $w(0, \beta_0)$.

In the calculation of the reweighting, it is possible to combine several ensembles obtained from different parameter sets, for instance multi-ensemble reweighting [22–24] or multi-histogram method [25]. Although those elaborated techniques are favorable to achieve better overlap, the reweighting with single ensemble is visible to understand the consistency between the Taylor expansion and reweighting. Thus, we use single ensemble reweighting for one target point.

The pressure is given by

$$\frac{\delta p}{T^4} = \left(\frac{N_t}{N_s} \right)^3 \ln \frac{\langle R(\mu, \beta)_{(0, \beta_0)} \rangle_0}{\langle R(0, \beta)_{(0, \beta_0)} \rangle_0}. \quad (2.10)$$

The quark number density and susceptibility are obtained from Eqs. (2.4) and (2.9).

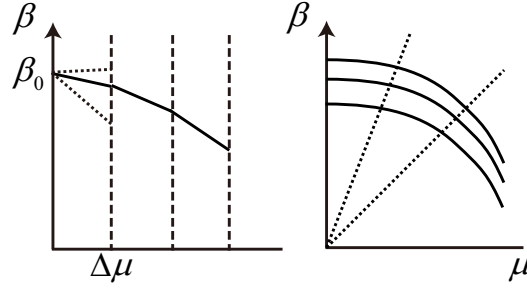


Figure 1. The determination of reweighting line and calculation of observables such as EoS. Left: First, the simulation point $(0, \beta_0)$ is fixed. The value of β minimizing X is determined for each μ . Right : Results from several reweighting lines are collected to obtain thermodynamical quantities for a given μ/T .

2.3 Overlap problem and reweighting line

The expectation value $\langle O \rangle$ given in Eq. (2.9) would be independent of the location of the simulation point $(0, \beta_0)$ in the parameter space, if a sufficiently large number of measurements is considered. In practice, $\langle O \rangle$ depends on $(0, \beta_0)$ in simulations with a finite number of samples. The problem arises from the fluctuation of the reweighting factor [12, 18]. It was found [8] that a better overlap can be obtained by using multiple parameters as reweighting parameters and by changing them appropriately.

Let X the fluctuation of the reweighting factor,

$$X(\mu, \beta) = \langle (R - \langle R \rangle_0)^2 \rangle_0. \quad (2.11)$$

Here we suppress the arguments of $R(\mu, \beta)_{(0, \beta_0)}$ and describe it as R . The condition for the parameter change is to keep the fluctuation X small.

Under the change of the parameters $(\mu, \beta) \rightarrow (\mu + \Delta\mu, \beta + \Delta\beta)$ with a fixed β_0 , the change of X is given as $\delta X = \langle R\delta R \rangle_0 - \langle R \rangle_0 \langle \delta R \rangle_0$. The fluctuation minimum condition $\delta X = 0$ gives

$$\frac{\langle R\delta R \rangle_0}{\langle R \rangle_0} = \langle \delta R \rangle_0. \quad (2.12)$$

By definition, the left hand side is given by

$$\frac{\langle R\delta R \rangle_0}{\langle R \rangle_0} = \langle \delta R \rangle = \frac{1}{Z} \int \mathcal{D}U \delta R w(\mu, \beta), \quad (2.13a)$$

and the right hand side is given by

$$\langle \delta R \rangle_0 = \frac{1}{Z} \int \mathcal{D}U \delta R w(0, \beta_0). \quad (2.13b)$$

Equation (2.12) is satisfied if the two weights are equal, $w(\mu, \beta) = w(0, \beta_0)$. This is realized if the target point and simulation point are coincide or if the number of configurations are sufficiently large. Instead of the global minimum, we choose the value of β that minimizes X for each value of μ . The

procedure is illustrated in Fig. 1. It was pointed out in Ref. [12] that the phase fluctuation of R can not be canceled by MPR procedure, because the gauge part of R is real. In this work, we limit our analysis to regions where the phase fluctuation is small.

The determination of the reweighting line requires the determinant evaluation for many parameter sets. In the present work, the use of the reduction formula makes this procedure easier. However, it would be useful to derive an easier way to find the reweighting line. The deviation of the reweighting factor δR for small $\Delta\mu$ and $\Delta\beta$ is given by

$$\delta R(\mu, \beta) = \frac{\partial R}{\partial(\mu/T)} \frac{\Delta\mu}{T} + \frac{\partial R}{\partial\beta} \Delta\beta. \quad (2.14)$$

Substitution of Eq. (2.14) into Eq. (2.12) gives

$$\left(\left\langle \frac{\partial R}{\partial(\mu/T)} \right\rangle - \left\langle \frac{\partial R}{\partial(\mu/T)} \right\rangle_0 \right) \frac{\Delta\mu}{T} = - \left(\left\langle \frac{\partial R}{\partial\beta} \right\rangle - \left\langle \frac{\partial R}{\partial\beta} \right\rangle_0 \right) \Delta\beta. \quad (2.15)$$

This gives the reweighting line. Note that $\langle \cdot \rangle$ is replaced with $\langle \cdot \rangle_0$ according to Eq. (2.9). It can be simplified further

$$\Delta\beta = \frac{\langle R^2 a \rangle_0 - \langle R \rangle_0 \langle Ra \rangle_0}{\langle R^2 b \rangle_0 - \langle R \rangle_0 \langle Rb \rangle_0} \frac{\Delta\mu}{T}, \quad (2.16a)$$

where

$$a = \frac{T \frac{\partial}{\partial\mu} [\det \Delta(\mu)]^{N_f}}{[\det \Delta(\mu)]^{N_f}}, \quad (2.16b)$$

$$b = S_G. \quad (2.16c)$$

Here we neglect a quark contribution to b : $\partial C_{\text{SW}}/\partial\beta$.

To find the reweighting line, one can use the equation of the reweighting line Eq. (2.15) or (2.16a) instead of calculating the fluctuation X for many parameter sets.

It was suggested in [12] that the equation of the reweighting line may correspond to the Clausius-Clapeyron equation in (p, T) plane. Equation (2.16a) has a similar correspondence. Especially, it is reduced to $\Delta\beta = (\langle n \rangle - \langle n \rangle_0) / (\langle S_G \rangle - \langle S_G \rangle_0) (\Delta\mu/T)$ in the vicinity of the simulation point.

2.4 Reduction formula for the Wilson fermion determinant

To consider the fluctuation minimum condition, we evaluate the quark determinant exactly by using the reduction formula for the Wilson fermion. Here, we briefly summarize the formula. For details, see [19–21]. For the reduction formula for staggered fermions, see [26, 27].

For the preparation of the reduction formula, we define block matrices

$$\begin{aligned} \alpha_i &= \alpha^{ab, \mu\nu}(\vec{x}, \vec{y}, t_i) \\ &= c_- B^{ab, \mu\sigma}(\vec{x}, \vec{y}, t_i) r_-^{\sigma\nu} - 2c_+ \kappa r_+^{\mu\nu} \delta^{ab} \delta(\vec{x} - \vec{y}), \end{aligned} \quad (2.17)$$

$$\begin{aligned} \beta_i &= \beta^{ab, \mu\nu}(\vec{x}, \vec{y}, t_i), \\ &= c_+ B^{ac, \mu\sigma}(\vec{x}, \vec{y}, t_i) r_+^{\sigma\nu} U_4^{cb}(\vec{y}, t_i) - 2c_- \kappa r_-^{\mu\nu} \delta(\vec{x} - \vec{y}) U_4^{ab}(\vec{y}, t_i). \end{aligned} \quad (2.18)$$

c_{\pm} are arbitrary scalar except for zero. $r_{\pm} = (r \pm \gamma_4)/2$ with the Wilson parameter r , where the reduction formula can be applied for arbitrary r . B is the Wilson fermion matrix without the temporal hopping terms. α_i describes a spatial hopping at t_i , while β_i describes a spatial hopping at t_i and a temporal hopping to the next time slice. They are independent of μ .

Using the block matrices, the reduction formula is given by

$$\det \Delta(\mu) = (c_+ c_-)^{-N/2} \xi^{-N_{\text{red}}/2} C_0 \det(\xi + Q), \quad (2.19a)$$

with

$$Q = (\alpha_1^{-1} \beta_1) \cdots (\alpha_{N_t}^{-1} \beta_{N_t}), \quad (2.19b)$$

$$C_0 = \left(\prod_{i=1}^{N_t} \det(\alpha_i) \right), \quad (2.19c)$$

where $\xi = \exp(-\mu/T)$, $N = 4N_c N_s^3 N_t$ and $N_{\text{red}} = N/N_t$. The rank of α_i and Q is given by N_{red} , which is reduced to $1/N_t$ compared to the rank of Δ . Furthermore, Q and C_0 are independent of μ , and the chemical potential is separated from the link variables.

The matrix Q describes propagations of quarks from the initial to final time slices [20], and is interpreted as a transfer matrix [19, 21]. Note that all the elements of Q uniformly contain N_t hopping terms in temporal direction, which enables to separate μ from Q . C_0 consists of the closed loops without temporal hopping. Then, C_0 is also independent of μ .

To obtain $\det \Delta$, we need to evaluate $\det(Q + \xi)$. Here we calculate the eigenvalues λ for $|Q - \lambda I| = 0$. Although the eigen problem requires large numerical cost, there is an advantage. Once we obtain λ , the quark determinant is the analytic function of μ . Then, the value of $\det \Delta(\mu)$ is obtained for arbitrary μ , which is useful for MPR. Other methods such as LU decomposition of $Q + \xi$ can be used instead of solving the eigenvalue problem for Q . In this case, we need to perform the LU decomposition for each μ .

With the eigenvalues of Q , we obtain

$$\det \Delta(\mu) = C_0 \xi^{-N_{\text{red}}/2} \prod_{n=1}^{N_{\text{red}}} (\lambda_n + \xi), \quad (2.20a)$$

$$= C_0 \sum_{n=0}^{N_{\text{red}}} c_n \xi^{n-N_{\text{red}}/2} = C_0 \sum_{n=-N_{\text{red}}/2}^{N_{\text{red}}} c_n \xi^n, \quad (2.20b)$$

where we set $c_{\pm} = 1$ for simplicity. Here we describe the determinant in two expressions: a product form Eq. (2.20a), and a summation form Eq. (2.20b). The second one denotes the fugacity expansion of the quark determinant, where fugacity coefficients c_n are polynomials of the eigenvalues λ_n [20].

2.5 Taylor expansion of EoS

Next we consider the Taylor expansion for the EoS. A noise method is often used to calculate Taylor coefficients. In this work, however, the derivatives are exactly obtained even for higher order terms by

using the reduction formula, which excludes errors caused by noise methods. As we will explain below, the thermodynamical quantities are obtained by using the eigenvalues of the reduced matrix both in the Taylor expansion and MPR methods. This provides an equal-footing basis for the comparison and consistency of the two methods.

The deviation of the pressure is expanded in powers of μ/T at $\mu = 0$ as follows

$$\frac{\delta p(\mu, T)}{T^4} = \sum_{n=2,4,\dots}^{\infty} c_n(T) \left(\frac{\mu}{T}\right)^n, \quad (2.21a)$$

where c_n are Taylor coefficients at $\mu = 0$ given by

$$c_n = \frac{1}{n!} \left(\frac{N_t}{N_s}\right)^3 T^n \left. \frac{\partial^n \ln Z_{GC}}{\partial \mu^n} \right|_{\mu \rightarrow 0}. \quad (2.21b)$$

The number density and number susceptibility are given by

$$\frac{n}{T^3} = \sum_{m=2,4,\dots}^{\infty} m \cdot c_m(T) \left(\frac{\mu}{T}\right)^{m-1}, \quad (2.22a)$$

$$\frac{\chi}{T^2} = \sum_{n=2,4,\dots}^{\infty} n(n-1) \cdot c_n(T) \left(\frac{\mu}{T}\right)^{n-2}. \quad (2.22b)$$

The n -th derivative of the grand partition function $Z_{GC}^{(n)} = (T\partial/\partial\mu)^n Z_{GC}$ is given by

$$\frac{Z_{GC}^{(n)}}{Z_{GC}} = \left\langle \frac{(T\partial/\partial\mu)^n [\det \Delta(\mu)]^{N_f}}{[\det \Delta(\mu)]^{N_f}} \right\rangle. \quad (2.23)$$

Derivatives of $\det \Delta$ are obtained from Eq. (2.20a) and Eq. (2.20b). Equation (2.20b) gives

$$T^k \frac{\partial^k}{\partial \mu^k} \det \Delta(\mu) = C_0 \sum_{n=0}^{N_{\text{red}}} (N_{\text{red}}/2 - n)^k c_n \xi^{n - N_{\text{red}}/2}, \quad (2.24)$$

which holds for arbitrary k . To derive derivatives of the product form Eq. (2.20a), we rewrite it as

$$\det \Delta(\mu) = \exp \left(\log(C_0 \xi^{-N_{\text{red}}/2} \prod_{n=1}^{N_{\text{red}}} (\lambda_n + \xi)) \right). \quad (2.25)$$

Then, derivatives are straightforwardly obtained by algebraic calculations. We use the product form, because it is easier to calculate than the summation form. The summation form is used for the check.

3 Result

3.1 Simulation setup

We consider the clover-improved Wilson fermions with $N_f = 2$ and RG-improved gauge action. Simulations were performed mostly on a $N_s^3 \times N_t = 8^3 \times 4$ lattice. We considered 29 values of β in

the interval $1.5 \leq \beta \leq 2.4$ for $N_s = 8$. Simulations on a $10^3 \times 4$ lattice were also performed for near β_{pc} to investigate the finite size effect. We considered 16 values in the interval $1.8 \leq \beta \leq 1.95$ for $N_s = 10$. The value of the hopping parameter κ was determined for each β by following the line of the constant physics with $m_{\text{PS}}/m_{\text{V}} = 0.8$ in Ref. [17]. The clover coefficient C_{SW} was determined by using a result obtained in the one-loop perturbation theory : $C_{\text{SW}} = (1 - 0.8412\beta^{-1})^{-3/4}$.

Gauge configurations were generated at $\mu = 0$ with the hybrid Monte Carlo simulations. The setup for the molecular dynamics was as follows: a step size $\delta\tau = 0.02$, number of the step $N_\tau = 50$ and length $N_\tau\delta\tau = 1$. The acceptance ratio was more than 90 % for $N_s = 8$ and 80 % for $N_s = 10$. HMC simulations were carried out for 11, 000 trajectories for each parameter set. For all the ensemble, the first 3,000 trajectories were removed as thermalization. The eigenvalues of the reduce matrix Q were calculated for each 20 HMC steps, and 400 sets of the eigenvalues were collected for each ensemble.

We show the estimation of computation time for the reduction formula, where we consider the following three steps ; calculation of the overall factor C_0 (2.19c), the construction of the matrix Q (2.19b) which includes the inverse matrices, the solving the eigenvalue problem. The details of the numerical procedure are as follows. LAPACK Library ZGETRF was used for the LU factorization of α_i and the calculation of C_0 . ZGETRI together with ZGETRF were used to obtain the inverse of α_i , and ZGEMM in BLAS was used, then Q was constructed. ZGESS in LAPACK was used to obtain eigenvalues of Q . NEC SX-9 at Osaka University was used in the calculations. Taking the average over 400 configurations, we evaluate the total time for these three procedure, and then further we take the average over some parameter sets. Estimated time was 750 sec for $8^3 \times 4$ and 4000 sec for $10^3 \times 4$. They are not scaled by V^3 , probably due to overhead time to construct Q . As a basis for comparison, we evaluated CPU time for 1000 HMC trajectories with the molecular dynamics setup explained above, where the standard CG algorithm was used. We spent about 61 000 sec for $8^3 \times 4$, and 112 000 sec for $10^3 \times 4$ in average. As a benchmark, the ratio (Time for 400 reduction) / (Time for 10, 000 HMC) is

$$\begin{aligned} \frac{750 \times 400}{61000 \times 10} &= 0.5 \quad (8^3 \times 4), \\ \frac{4000 \times 400}{112000 \times 10} &= 1.4 \quad (10^3 \times 4). \end{aligned}$$

The numerical cost of the reduction formula was almost the same order as that of 10, 000 HMC update in $8^3 \times 4$ or $10^3 \times 4$ lattice in the present calculation setup. If one performs the determinant calculation of the original Wilson matrix, the above quantity would become about $N_t^2 = 16$ times larger.

3.2 Fluctuation of the quark determinant

First, we investigate the fluctuation of the quark determinant. Figure 2 shows the scatter plot of $N_f \ln \det \Delta(\mu) / \det \Delta(0) = \ln R(\mu, \beta_0)_{(0, \beta_0)}$. We show the results for $\beta_0 = 1.8(T/T_{\text{pc}} \sim 0.93)$ and 1.9(1.08). The quark determinant shows different μ -dependence corresponding to the value of β_0 . It increases mainly in magnitude at $\beta_0 = 1.9$ (high T), while it increases in phase at $\beta_0 = 1.8$ (low T). Near $\beta_{\text{pc}}(\sim 1.86)$, the quark determinant fluctuates between low- T and high- T states.

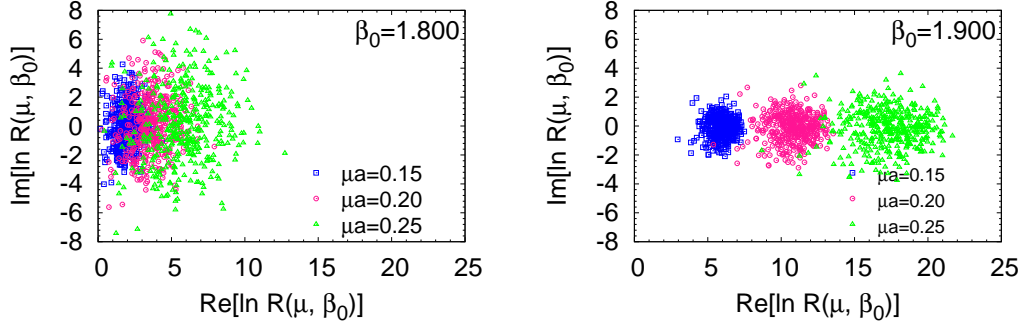


Figure 2. The scatter plot of the quark determinant on the complex plane.

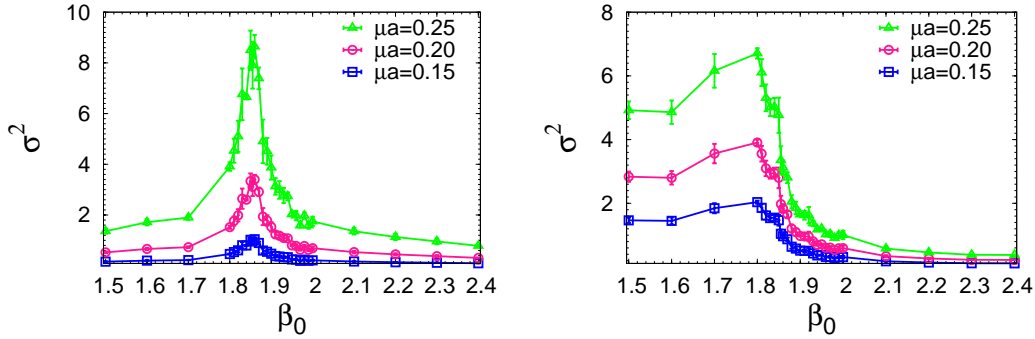


Figure 3. The fluctuation of the quark determinant as a function of β_0 . $\sigma^2 = \frac{1}{n} \sum_i (x_i - \bar{x})^2$, $\bar{x} = \frac{1}{n} \sum_i x_i$, where $x = \text{Re}[\ln R(\mu, \beta_0)_{(0, \beta_0)}]$ for left panel and $x = \text{Im}[\ln R(\mu, \beta_0)_{(0, \beta_0)}]$ for right panel.

Figure 3 illustrates the behavior of the fluctuation of the quark determinant defined as the standard deviation. The real part of $\ln R$, which is the power of $|R|$, shows a peak near the crossover transition β_{pc} , which is caused by the fluctuation between low- and high- T states. The peak causes the contamination of unimportant configurations and implies the severe overlap problem. The peak becomes prominent for $\mu a > 0.2$. Except for the vicinity of β_{pc} , the fluctuation is not so large compared to the present statistics at least for small μ , and therefore the overlap problem is not so severe.

For the imaginary part of $\ln R$, which is the phase of R , the fluctuation is large for near and below β_{pc} , and small at large β . It was pointed out [12] that the fluctuation of the phase of the reweighting factor is not suppressed by the MPR method because the gauge part is real. If the phase goes over $\pi/2$, the determinant changes the sign, and causes the sign problem. Adopting the standard deviation as a criterion, the onset of the problem is $\mu a \sim 0.2$ near β_{pc} . This imposes an applicable limit of MPR on the $8^3 \times 4$ lattice in the present simulation setup. We limit our analysis on the thermodynamical quantities up to $\mu a = 0.20$. Applicable range of MPR in the present work is smaller than that of staggered fermions investigated in Ref.[18]. This difference may be caused by small statistics.

The severity of the problems is roughly classified into three cases according to temperatures. At

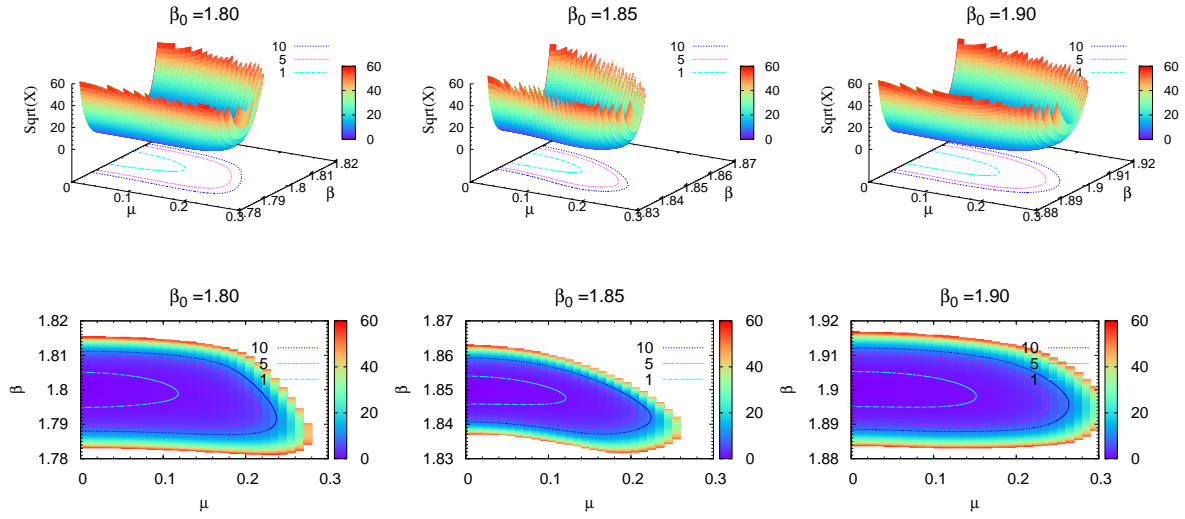


Figure 4. Fluctuation of the total reweighting factor (top panels) and its contour plot on the μ - β plane (bottom panels). The simulation points are $\beta_0 = 1.80, 1.85$ and 1.90 for left, middle and right panels respectively. Here we take the absolute values of the fluctuation $X = \langle |R - \langle R \rangle_0|^2 \rangle_0$.

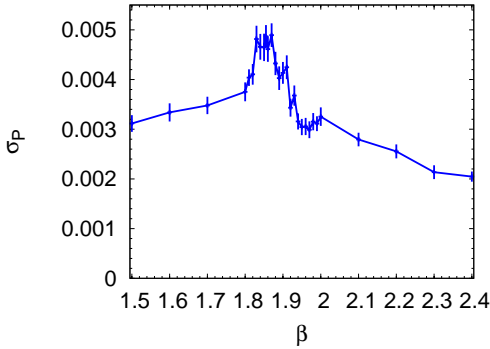


Figure 5. Variation of the plaquette distribution extracted from the Gaussian fit $f(P) = \exp(-(P - \langle P \rangle)^2 / (2\sigma_P^2))$ with P being the plaquette.

high temperatures, the fluctuation is small both for the real and imaginary parts, and the sign problem and overlap problem is not severe. Near β_{pc} , both the real and imaginary parts fluctuate rapidly. At low temperatures, the phase fluctuates rapidly, while the fluctuation of the real part is not so large.

3.3 Fluctuation of the reweighting factor and Reweighting line

Next, we consider the fluctuation of the reweighting factor X . Here we modify the condition to $X = \langle |R - \langle R \rangle_0|^2 \rangle_0$. It is an alternative choice to take the real part of R . In the calculation of thermodynamical quantities, we limit our study to the region where the fluctuation of the phase is small. Then, we can use either of the absolute value or real part.

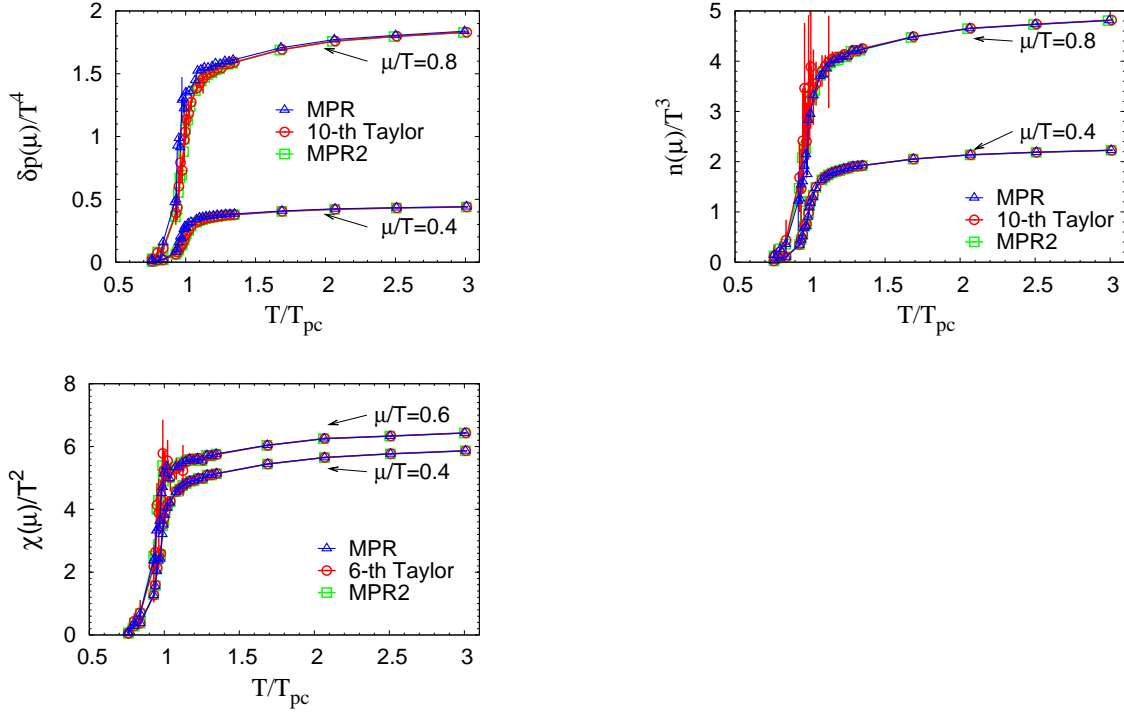


Figure 6. Thermodynamical quantities obtained from Taylor expansion (circle), MPR with the fluctuation minimum condition (triangle) and MPR with Eq. (2.16a) (square).

The contour plot of X in Fig. 4 illustrates how X increases in the shift of the parameters from simulation points. The shape of X is related to the distribution of the quark determinant and of the plaquette, see Figs. 3, 4 and 5. The rapid fluctuation of the plaquette makes the valley steep in β direction, while that of the quark determinant makes the valley steep in μ direction.

Near β_{pc} , both the plaquette and the quark determinant fluctuate rapidly, which makes the valley steep and results in narrowing the small fluctuation domain. For this case, the valley curves downward, and X remains small due to the cancel of the contributions of the plaquette and quark determinant.

To avoid the overlap problem, the fluctuation X needs to be suppressed. The reweighting line is taken along the valley of X for each ensemble.

3.4 Consistency of MPR and Taylor expansion for EoS

Thermodynamical quantities are shown in Fig. 6. To obtain the values of T from β , we use the data in Ref. [17]. The EoS and number density for the Taylor expansion contains up to tenth order, while the susceptibility up to sixth order. The Taylor coefficients given in Eq. (2.21b) are shown in Fig. 7. MPR and Taylor expansion methods are almost consistent up to $\mu/T \sim 0.8$ for the EoS and quark number density. For the susceptibility, the consistency holds for up to $\mu/T \sim 0.6$, while errors become large for $\mu/T > 0.6$ particularly near T_{pc} .

Figure 6 also shows the results obtained from the equation of the reweighting line given in Eq. (2.16a). It turns out that the equation of the reweighting line is almost consistent with the fluctuation minimum condition. Next, we see the Taylor coefficients. c_2 and c_4 are consistent with those

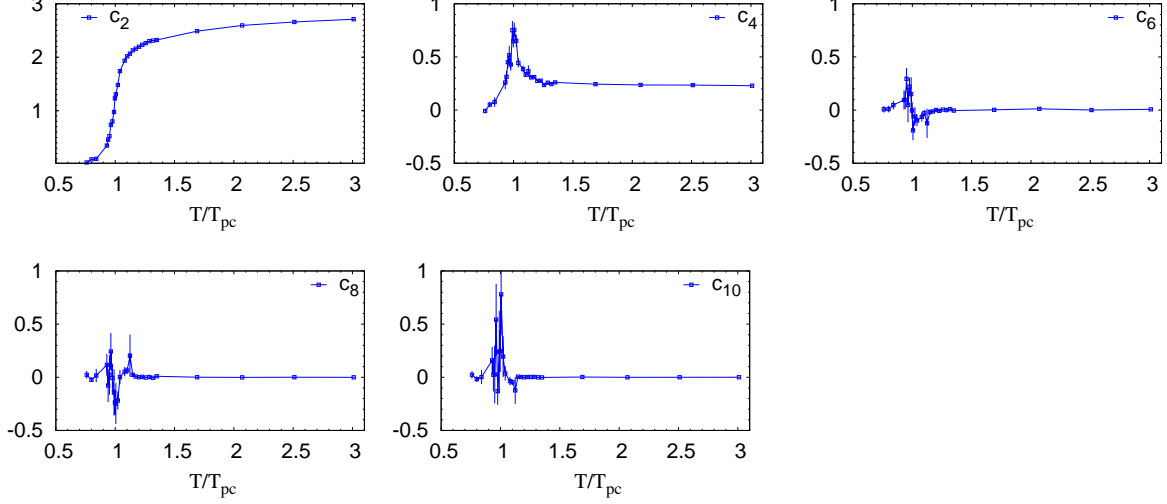


Figure 7. Taylor coefficients c_n , ($n = 2, \dots, 10$).

obtained by the same action and larger lattice $16^3 \times 4$ [17] probably due to the crossover nature of the transition at small μ . The Taylor series converges up to $\mathcal{O}((\mu/T)^4)$ for high T , which is consistent with the expected behavior from free-quark-gluon picture. On the other hand, the convergence is slow near and below T_{pc} . c_n oscillates and the number of the oscillation increases with n . This behavior was observed in a Polyakov-quark-meson model with $2 + 1$ flavors [28]. Statistical errors become larger for higher coefficients. The inclusion of c_8 and c_{10} causes large errors for the number susceptibility χ . The errors become significant for large $\mu/T \sim 1$ for EoS and $\mu/T \sim 0.8$ for χ .

The comparison with a noise method for c_2 is shown in Fig. 8, where the trace of an operator A is calculated by $\text{tr}A = (N_r^{-1}) \sum_{i=1}^{N_r} (v^{(i)})^* A v^{(i)}$, where $v^{(i)}$, ($i = 1, 2, \dots, N_r$) is noise vectors and N_r is the number of the noise vectors. We employ the noise vectors for all the indices, i.e., the color, Dirac and coordinate space, $N_r^{-1} \sum_{i=1}^{N_r} v_{a,\alpha,\vec{x}}^{(i)} (v_{b,\beta,\vec{y}}^{(i)})^* = \delta_{a,b} \delta_{\alpha,\beta} \delta_{\vec{x},\vec{y}}$. It turns out that 400 noise vectors are almost enough for the noise method to reproduce c_2 of the reduction formula both in the average value and errorbar. Note that the number of the noise may be reduced further by the improvement of the noise methods. For each measurement, the noise method slowly converges according to $O(1/\sqrt{N_r})$, and large number of noise vectors are needed to reproduce the result of the reduction formula. Taking the ensemble average improves the convergence, which allows to use fewer number of the noise vectors. The computational time for one measurement of c_2 with BiCGStab algorithm was about 240, 320 and 400 sec for $N_r = 600, 800$ and 1000, respectively, while the time for the reduction formula was about 1000 sec. For c_2 , the noise method is several times faster than the reduction formula. On the other hand, the reduction formula provides higher order coefficients with small additional calculation. For higher-order Taylor coefficients, the reduction formula becomes

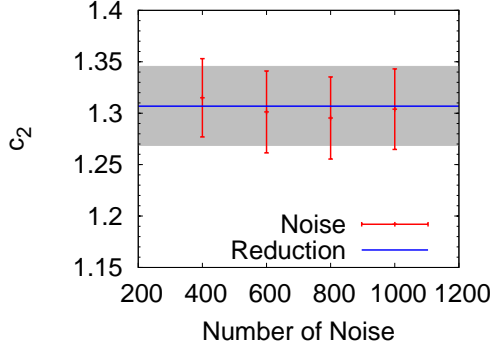


Figure 8. The Taylor coefficient c_2 at $T/T_{\text{pc}} = 1$ ($\beta = 1.86$) obtained from the noise method with different number of noise vectors. The horizontal line is the value obtained from the reduction formula, where the errorbar is denoted by the gray region.

faster than the noise method. However, it should be noted that the reduction formula is limited to small lattice size.

Here we comment on the difference of the errorbars, and on the applicable limit of the two approaches. In our approach, the Taylor expansion and MPR methods are obtained from the same quantities, i.e., the eigenvalues of the reduced matrix. The thermodynamical quantities are defined in Eq. (2.4) for the MPR method and in Eq. (2.22) for the Taylor expansion method. In the Taylor expansion, the numerical errors of the thermodynamical quantities mainly come from higher-order Taylor coefficients, see Fig. 7. The derivatives of the pressure, n/T^3 and χ/T^2 , are sensitive to higher c_n because of the multiplicative factors in Eq. (2.22). For instance, the tenth term c_{10} is enhanced by the factor 10 and 10×9 in n/T^3 and χ/T^2 , respectively. This is the origin of the large errors in Fig. 6 and restricts the applicable limit of the Taylor expansion. For large μ/T , higher-order coefficients become important, and as a consequence, the Taylor expansion of the EoS is breakdown, which happens at $\mu/T \sim 0.8$ near $T \sim T_{\text{pc}}$ for $\delta p/T^4$.

In the MPR method, the numerical errors come from statistical fluctuation of the reweighting factor and observables. The MPR requires only the first and second derivative terms of the fermion determinant in the calculation of n/T^3 and χ/T^2 , see Eq. (2.4). The fluctuation of the reweighting factor is suppressed if the parameters change along the small fluctuation region, see Fig. 4. The major origin of the difference in the errorbars is the calculation of higher-order derivative terms, which is contained only in the Taylor expansion method and not in the MPR method 7. As shown in Fig. 3, the fluctuation of the imaginary part of the reweighting factor becomes large about $\mu a \sim 0.2$ ($\mu/T \sim 0.8$) near $T \sim T_{\text{pc}}$, which is also near the edge of the small fluctuation domain in Fig. 4. Thus, the applicable range of the two methods are consistent, although the numerical errors appear in different way. This is natural consequence of that the fermion determinant and its derivatives are given by the same quantities λ_n of the reduced matrix, hence their fluctuations are correlated.

Thus, the MPR and Taylor expansion methods suffer from the different difficulties. Hence, their consistency implies that the truncation error of the Taylor expansion method and overlap problem of

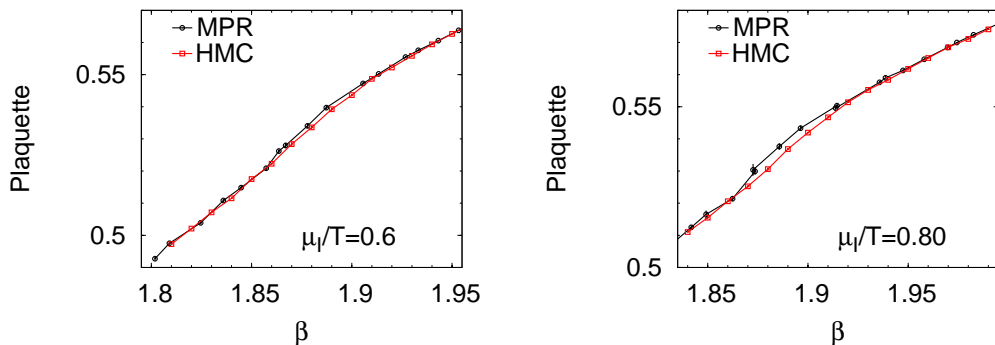


Figure 9. Plaquette at imaginary chemical potential. The results for HMC were obtained from the direct simulations at μ_I , while those for MPR were obtained from the simulations at $\mu = 0$ with MPR method.

MPR are not serious and that the obtained thermodynamical quantities are reliable in these regions in spite of these difficulties.

Note that the fluctuation of imaginary part of the reweighting factor depends on the lattice volume, and the applicable range of the reweighting becomes smaller as the lattice volume increases. We will discuss this point later.

3.5 Consistency with imaginary chemical potential approach

Since the comparison of MPR and Taylor expansion was done by using the same configurations, it may happen that both the methods are breakdown with same systematic errors. For further check, we consider the plaquette at imaginary chemical potential μ_I and compare the results with direct simulations. The consistency among several finite density lattice simulations was studied for staggered fermions in Ref. [23]. The results are shown in Fig. 9, where the data of direct simulations are taken from [29]. MPR is almost consistent with the direct simulation up to $\mu_I a = 0.20$, although they are obtained from different configurations. A small disagreement appears for $\mu_I a = 0.20$ and it becomes larger for larger μ_I . This agreement shows that the overlap problem caused by the real part of the reweighting factor is not severe up to $\mu_I/T = 0.8$. Note that the small error owes to the absence of the phase of the determinant at μ_I and that this consistency is irrelevant of the problem caused by the imaginary part of R .

3.6 Finite size effects

Finally, we consider the finite size effects. The fluctuation of the quark determinant is shown for $N_s = 8$ and $N_s = 10$ in Figs. 3 and 10, where two calculations were performed in the same number of statistics. The fluctuations are almost proportional to the spatial volume $10^3/8^3 \sim 2$ for both the power and phase. This implies a well known result [1] that the severity of the overlap problem is proportional to $O(\exp(V))$. In particular, the phase fluctuation goes over $\pi/2$ at about $\mu a \sim 0.15$ near and below β_{pc} , which imposes the applicable limit of MPR on this lattice size with the given statistics.

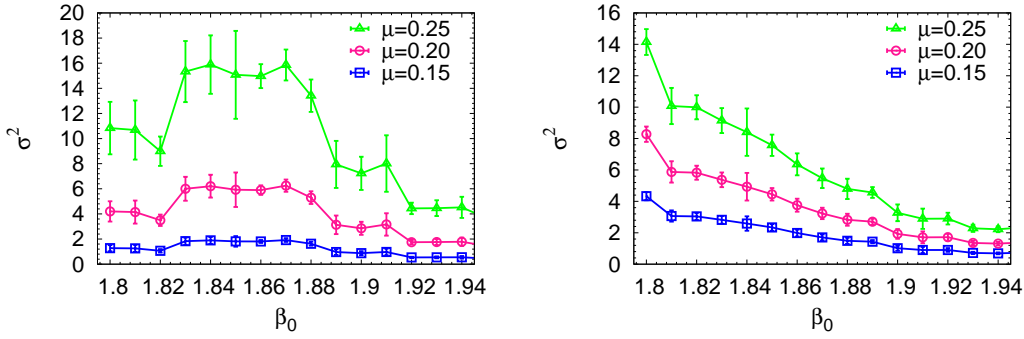


Figure 10. The fluctuation of the quark determinant on $10^3 \times 4$. σ is given in the caption of Fig. 3.

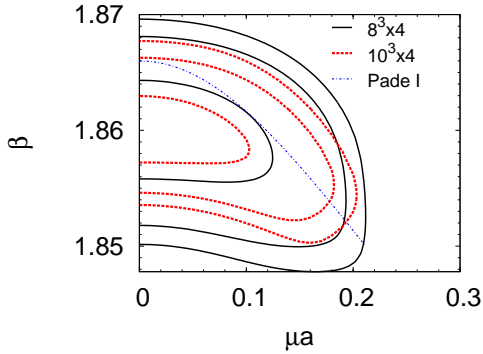


Figure 11. Contour lines of the fluctuation of the reweighting factor. The solid and dashed lines are for $8^3 \times 4$ and $10^3 \times 4$. The pseudo critical line (Padé I) is obtained in [29].

In Fig. 11, we show contour lines of X for $8^3 \times 4$ and $10^3 \times 4$. The dotted line (Padé I) shows the pseudo critical line obtained by the analytic continuation from imaginary chemical potential on the $8^3 \times 4$ [29]. The contour lines shrink due to the increase of N_s , the applicable range of the MPR becomes smaller for large lattice size. In order to extend the applicable range of MPR, it is required to increase statistics corresponding to the lattice size.

On the other hand, the shape of the contour line is similar for $N_s = 8$ and $N_s = 10$ in a sense that the fluctuation rapidly increases if the phase transition line is acrosed. It was shown in Ref. [12] that in a system with a first order phase transition, the fluctuation of the reweighting factor is minimum along the phase transition line, on a assumption that the fluctuation is dominated by the flip-flop between the two phases on the first order phase transition line. Although the phase transition is crossover, the fluctuation near T_{pc} is dominant by the one between hadron and QGP phases. Then, the direction of the reweighting line is insensitive to N_s . We have also confirmed that the EoS are not affected by the finite size effects up to $\mu a = 0.2$, and number density and susceptibility up to $\mu a = 0.10$. As long as we consider the parameter region with the small fluctuation, EoS, number density and susceptibility are insensitive to the lattice size, probably owing to the crossover nature of

the deconfinement transition.

4 Summary

We have studied thermodynamical properties of QCD at nonzero quark chemical potential μ using the MPR and Taylor expansion methods with a careful attention on the consistency of the MPR and Taylor expansion.

Simulations were performed on the $8^3 \times 4$ lattice with an intermediate quark mass region $m_{\text{ps}}/m_V \sim 0.8$ with the clover-improved Wilson fermion and RG-improved gauge action. The HMC simulation was done for 11 000 trajectories. Although the lattice size is small, the quark determinant was evaluated exactly by using the reduction formula for the Wilson fermion determinant. The eigenvalues of the reduced matrix were calculated for 400 configurations.

Rapid fluctuation of the reweighting factor is known to cause the breakdown of MPR. To avoid the difficulty, we investigated the fluctuation of the reweighting factor. We have confirmed that the fluctuation of the reweighting factor is enough small up to $\mu a \sim 0.2$ both in the magnitude and phase. For the Taylor expansion, we evaluated the Taylor coefficients up to tenth order. Then, we have calculated the EoS, quark number density and quark number susceptibility. The MPR and Taylor expansion methods show a good agreement for the EoS and number density up to $\mu/T \sim 0.8$ and number susceptibility up to $\mu/T \sim 0.6$.

One of the difficulty of the MPR method is the determination of the reweighting line, since it needs the calculation of the determinant for many parameter sets. We have derived the equation of the reweighting line and showed that the equation of the reweighting line is consistent with the fluctuation minimum condition for the calculation of the thermodynamical quantities. Using the equation of the reweighting line, one can avoid the determinant evaluation to search the fluctuation minimum line.

To see how the obtained results are affected by finite size effects, we have compared $8^3 \times 4$ and $10^3 \times 4$. As expected, the fluctuation of the quark determinant increases as the volume becomes larger. In particular, the large fluctuation of the phase makes the applicable parameter range of MPR smaller. The phase fluctuation goes over $\pi/2$ for $\mu a \sim 0.15$ on the $10^3 \times 4$ lattice. As long as we consider the parameter region with the small fluctuation, EoS, number density and susceptibility are insensitive to the lattice size, probably owing to the crossover nature of the deconfinement transition.

The Taylor expansion and MPR methods have different advantage and difficulty. The MPR method suffer from the fluctuation of the reweighting factor, while it is free from truncation error of Taylor series. On the other hand, the Taylor expansion suffer from the truncation error, while it does not contain the reweighting factor. Thus, the obtained agreement between the two methods implies that the overlap problem for the MPR and truncation error for the Taylor expansion method are negligible for small μ and that the thermodynamical quantities are reliable for these errors.

Although the present analysis is limited to small μ region, CEP may be located on a small or moderate μ region. The consistency observed here would be useful information for the studies of the CEP search.

Acknowledgment

This work was supported by Grants-in-Aid for Scientific Research 20340055 and 20105003. The simulation was performed on NEC SX-8R at RCNP, and NEC SX-9 at CMC, Osaka University.

References

- [1] P. de Forcrand, *Simulating QCD at finite density*, *PoS LAT2009* (2009) 010, [[arXiv:1005.0539](#)].
- [2] S. Muroya, A. Nakamura, C. Nonaka, and T. Takaishi, *Lattice QCD at finite density: An Introductory review*, *Prog.Theor.Phys.* **110** (2003) 615–668, [[hep-lat/0306031](#)].
- [3] C. Schmidt, *Lattice QCD at finite density*, *PoS LAT2006* (2006) 021, [[hep-lat/0610116](#)].
- [4] A. Ferrenberg and R. Swendsen, *New Monte Carlo Technique for Studying Phase Transitions*, *Phys.Rev.Lett.* **61** (1988) 2635–2638.
- [5] I. M. Barbour and A. J. Bell, *Complex zeros of the partition function for lattice QCD*, *Nucl. Phys.* **B372** (1992) 385–402.
- [6] I. M. Barbour, S. E. Morrison, E. G. Klepfish, J. B. Kogut, and M.-P. Lombardo, *Results on finite density QCD*, *Nucl. Phys. Proc. Suppl.* **60A** (1998) 220–234, [[hep-lat/9705042](#)].
- [7] Z. Fodor and S. Katz, *A New method to study lattice QCD at finite temperature and chemical potential*, *Phys.Lett.* **B534** (2002) 87–92, [[hep-lat/0104001](#)].
- [8] Z. Fodor and S. Katz, *Lattice determination of the critical point of QCD at finite T and mu*, *JHEP* **0203** (2002) 014, [[hep-lat/0106002](#)].
- [9] Z. Fodor, S. Katz, and K. Szabo, *The QCD equation of state at nonzero densities: Lattice result*, *Phys.Lett.* **B568** (2003) 73–77, [[hep-lat/0208078](#)].
- [10] Z. Fodor and S. Katz, *Critical point of QCD at finite T and mu, lattice results for physical quark masses*, *JHEP* **0404** (2004) 050, [[hep-lat/0402006](#)].
- [11] Z. Fodor and S. Katz, *The Phase diagram of quantum chromodynamics*, [arXiv:0908.3341](#).
- [12] S. Ejiri, *Remarks on the multiparameter reweighting method for the study of lattice QCD at nonzero temperature and density*, *Phys.Rev.* **D69** (2004) 094506, [[hep-lat/0401012](#)].
- [13] C. Allton, S. Ejiri, S. Hands, O. Kaczmarek, F. Karsch, *et. al.*, *The QCD thermal phase transition in the presence of a small chemical potential*, *Phys.Rev.* **D66** (2002) 074507, [[hep-lat/0204010](#)].
- [14] C. Allton, S. Ejiri, S. Hands, O. Kaczmarek, F. Karsch, *et. al.*, *The Equation of state for two flavor QCD at nonzero chemical potential*, *Phys.Rev.* **D68** (2003) 014507, [[hep-lat/0305007](#)].
- [15] C. Allton, M. Doring, S. Ejiri, S. Hands, O. Kaczmarek, *et. al.*, *Thermodynamics of two flavor QCD to sixth order in quark chemical potential*, *Phys.Rev.* **D71** (2005) 054508, [[hep-lat/0501030](#)].
- [16] R. Gavai and S. Gupta, *The Critical end point of QCD*, *Phys.Rev.* **D71** (2005) 114014, [[hep-lat/0412035](#)].
- [17] **WHOT-QCD Collaboration** Collaboration, S. Ejiri *et. al.*, *Equation of State and Heavy-Quark Free Energy at Finite Temperature and Density in Two Flavor Lattice QCD with Wilson Quark Action*, *Phys.Rev.* **D82** (2010) 014508, [[arXiv:0909.2121](#)].

- [18] F. Csikor, G. Egri, Z. Fodor, S. Katz, K. Szabo, *et. al.*, *Equation of state at finite temperature and chemical potential, lattice QCD results*, *JHEP* **0405** (2004) 046, [[hep-lat/0401016](#)].
- [19] A. Borici, *Reweighting with stochastic determinants*, *Prog. Theor. Phys. Suppl.* **153** (2004) 335–339.
- [20] K. Nagata and A. Nakamura, *Wilson Fermion Determinant in Lattice QCD*, *Phys.Rev.* **D82** (2010) 094027, [[arXiv:1009.2149](#)].
- [21] A. Alexandru and U. Wenger, *QCD at non-zero density and canonical partition functions with Wilson fermions*, *Phys.Rev.* **D83** (2011) 034502, [[arXiv:1009.2197](#)].
- [22] A. M. Ferrenberg and R. H. Swendsen, *Optimized Monte Carlo analysis*, *Phys.Rev.Lett.* **63** (1989) 1195–1198.
- [23] S. Kratochvila and P. de Forcrand, *The canonical approach to finite density QCD*, *PoS LAT2005* (2006) 167, [[hep-lat/0509143](#)].
- [24] P. de Forcrand and S. Kratochvila, *Finite density QCD with a canonical approach*, *Nucl. Phys. Proc. Suppl.* **153** (2006) 62–67, [[hep-lat/0602024](#)].
- [25] **WHOT-QCD collaboration** Collaboration, Y. Nakagawa *et. al.*, *Histogram method in finite density QCD with phase quenched simulations*, [arXiv:1111.2116](#).
- [26] P. E. Gibbs, *THE FERMION PROPAGATOR MATRIX IN LATTICE QCD*, *Phys. Lett.* **B172** (1986) 53.
- [27] A. Hasenfratz and D. Toussaint, *Canonical ensembles and nonzero density quantum chromodynamics*, *Nucl. Phys.* **B371** (1992) 539–549.
- [28] B.-J. Schaefer, M. Wagner, and J. Wambach, *QCD thermodynamics with effective models*, *PoS CPOD2009* (2009) 017, [[arXiv:0909.0289](#)].
- [29] K. Nagata and A. Nakamura, *Imaginary Chemical Potential Approach for the Pseudo-Critical Line in the QCD Phase Diagram with Clover-Improved Wilson Fermions*, *Phys.Rev.* **D83** (2011) 114507, [[arXiv:1104.2142](#)].